Adapting a JEM-2100F for Magnetic Imaging by Lorentz TEM

Amit Kohn and Avihay Habibi

Department of Materials Engineering and the Ilse Katz Institute for Nanoscale Science and Technology, Ben-Gurion University of the Negev

Lorentz TEM enables to map quantitatively magnetic induction fields in the sample. A specifically designed objective lens, a coherent electron source, and a biprism filament can achieve magnetic imaging at the nanometer scale through off-axis electron holography experiments. However, this equipment is specialized and therefore not suited to many microscopy labs. In this article, we describe an adaptation of a conventional JEM-2100F for Lorentz phase microscopy, namely Fresnel-contrast imaging. Since a biprism filament is installed on this microscope, we evaluate the capabilities of the Fresnel-contrast magnetic imaging. We show that a relatively simple and low-cost adaptation enables quantitative magnetic and electrostatic mapping on a conventional TEM.

Introduction

The development of new magnetic materials, e.g. for information storage devices, requires the characterization of the structural, chemical, electronic and magnetic properties of these materials at the nanometer and even atomic scale. Transmission electron microscopy (TEM) is a versatile tool for materials characterization that contributes significantly towards all these goals [1]. Amongst the capabilities of electron microscopy is the so-called 'Lorentz TEM', which enables to map quantitatively the magnetic and electrostatic fields of the material at the nanometer scale. In addition, *in situ* experiments are performed to image the micromagnetic structure while subjecting the specimen to magnetic and electrical fields [2, 3].

A combination of a specifically designed objective lens, a coherent electron source, and a biprism filament enables magnetic mapping at a spatial resolution in the nanometer scale, e.g References [4,5]. However, such a combination is specialized and expensive, therefore not suited for most electron microscopy labs.

In this report, we describe an adaptation of a conventional JEM-2100F for Lorentz TEM, and show that achieving Fresnel-contrast imaging is straightforward. Since this microscope has a coherent electron source, and is equipped with a biprism filament, we also report on the off-axis holography characteristics under these conditions. Electron holography enabled us to examine the quantitative capabilities of Fresnel-contrast imaging in the modified TEM for magnetic mapping.

The outline of the paper is as follows: The requirements for adapting a microscope for Lorentz TEM are presented. Following this, the modifications of the JEM-2100F are described. The relevant optical parameters of the adapted microscope are then characterized. We present an example of magnetic imaging both in Fresnel-contrast, and electron holography in order to demonstrate and evaluate the quantitative capability of the adapted microscope. Finally, we show that low-angle electron diffraction is also possible using free-lens control.

Requirements

The initial requirement for performing Lorentz TEM is to position the sample in a region free from external magnetic fields. Many samples of interest are based on soft magnetic materials, namely their coercivity is under 50 Oe. Consequently, the magnetic field in the region of the sample should be less than several Oe. In addition, during the insertion of the holder through the load-lock, the sample should not be subjected to significant stray magnetic fields from the column. Therefore, the first stage is to close the current supply to the objective lens, and use the objective mini-lens instead (calculated focal length of 42 mm, 10% accuracy).

Lorentz TEM is often used for *in situ* experiments. A typical research interest is to examine the development of the micromagnetic structure with applied external field. A basic method to achieve this is by using the objective lens to generate a magnetic field along the optic axis. The sample is then tilted to apply both an

Be'er-Sheva 84105, Israel

E-mail: akohn@bgu.ac.il

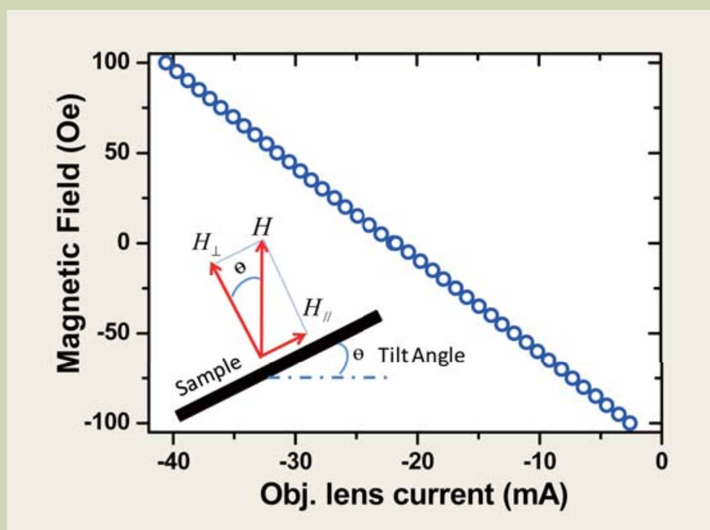

Fig. 1 The magnetic field along the optic-axis of the microscope as a function of applied current to the objective lens. Inset: tilting the sample enables to apply a magnetic field also in the plane of a thin film.

in-plane and out-of-plane magnetic field (see inset of **Figure 1**). Tilting of the sample is necessary because for soft magnetic materials, the magnetic moments reside in-plane. In recent years, there is increased technological interest in perpendicular magnetic media, which is based on hard magnetic materials. Here, there is an advantage to apply large magnetic fields (possible up to approximately 2 Tesla using the objective lens) along the optical axis, perpendicular to the sample plane.

When using the objective mini-lens, the magnification range should enable magnetic mapping at nanometer resolution: A pixel calibration of the CCD at around 1 nm is sufficient for Fresnel-contrast imaging.

Finally, the aberrations of the microscope should be characterized in order to evaluate the imaging capabilities of the microscope. For Lorentz TEM in a conventional microscope, the relevant aberrations are mainly the spherical aberration, C_S, and the defocus distance. Measuring C_S and calibrating the defoci distances can then enable quantitative analysis of the Fresnel-contrast images by comparison to image simulations.

Adaptation and characterization

The first step of the adaptation was to extend the magnification range of the objective mini-lens. Lens settings were obtained from JEOL to extend the magnification from the usual maximum setting of 6kX up to 40kX. The latter magnification is sufficient for the spatial resolution required both in Fresnel-contrast imaging and for electron holography. At a nominal magnification of 40kX, the pixel calibration is approximately 0.25 nm on a 2048 × 2048 Gatan Ultrascan Charge-Coupled-Device (CCD).

At this stage, the residual field was measured with a Hall probe that was incorporated onto a sample holder. The typical residual magnetic field measured on the sample was approximately 190 Oe. While this residual field is small compared to the regular operation of the objective lens, it will saturate most soft magnetic materials.

Reduction of the remnant field is necessary, and can be achieved by applying a current on the objective lens. Setting 34.4 mA to this lens decreased the residual field to approximately 0.1 Oe. The required current can be reduced by degaussing the objective lens, namely cycling the applied current on the objective lens in decreasing magnitude from 1 Ampere. After the degaussing procedure (approximately 2 minutes), a reduced current of under 22 mA is applied to reduce the remnant field to approximately 0.1 Oe.

The stability of this low field was examined to determine the duration of experiments that can be undertaken. The residual field increased at a rate of 0.2-0.3 Oe per hour, meaning that experiments spanning 4 hours can be conducted while ensuring that the residual field at the sample is less than 1 Oe. The stability of the residual field was examined with the change of magnification. Starting from the highest magnification setting of 40kX, the field increased approximately linearly up to 0.5 Oe when reducing the magnification down to 8kX. When the magnification setting was further reduced, the residual field increased to over 4 Oe at 6kX, further increasing to above 6 Oe at the lowest magnifications. A similar change of the residual field was measured when starting at low magnifications and then increasing the magnification. This observation can be explained by the new lens setting of the objective mini-lens. Since the magnification range was increased beyond 6kX, the current applied to the objective mini-lens changes, which results in a change in the magnetic field applied to the sample.

The residual field was also examined with the change of current or defocusing of the objective mini-lens. This measurement is relevant for Fresnel contrast imaging, where the typical defoci distances span from tens to hundreds of micrometers. For underfocus, the field increased to over 0.2 Oe, 0.3 Oe, and 0.4 Oe up to defoci distances of 100 μm, 400 μm, and 900 μm, respectively. For overfocus, the residual field was stable, below 0.3 Oe, up to a defocus distance of 900 μm.

We conclude that a residual field of under 1 Oe can be maintained in the sample region with the use of the objective mini-lens over a wide range of magnifications and defoci distances, and during experiments conducted for several hours.

After reducing the residual field, the magnetic field was measured when removing and inserting the sample holder with the Hall probe. A maximum field of 2 Oe was measured during this process. Therefore, the insertion of the sample is not expected to affect the micromagnetic structure of the sample.

As previously explained, the objective lens can be used to apply a magnetic field on the sample. In Figure 1, the field, measured in the applied current range of approximately 40 mA to 2 mA is presented, equivalent to magnetic fields spanning between -100 to +100 Oe. This result shows a linear response, which can be further extended by increasing the current on the objective lens.

The next stage is to characterize the aberrations of this Lorentz setup. For magnetic imaging and phase reconstruction at the nanometer scale resolution, the two important aberrations to measure are the spherical aberration, C_S, and the defocus distance. Calibrating the defoci distances as a function of the objective mini-lens current is also required for choosing the correct Fresnel-contrast conditions and quantifying the results.

The two aberrations were measured using the methodology outlined in Reference [6]. **Figure 2**(a) shows the calibration of the defoci distances. The minimum defocus step is 3.02 ± 0.01 µm. This focal step is small enough for Fresnel contrast imaging. However, when finer control is needed, for example to achieve the Gaussian defocus, then the z-axis of the stage can mechanically translate the sample by steps of 0.3 µm (verified by the above mentioned methodology). Figure 2(b) shows the measured C_S for the various defoci distances. The average measurement of the spherical aberration is 4.61 ± 0.17 m, while the chromatic aberration was calculated to be 87 mm. The point resolution of this low magnification, Lorentz set-up is therefore approximately 2 nm.

Figure 3 is a comparison of bright-field TEM images of gold nanoparticles, sputter-deposited on an amorphous carbon film, obtained with the adapted Lorentz mode (left) and with the conventional TEM imaging (right). While degradation in the image quality is observed, a spherical aberration of several meters still enables imaging with nanometer resolution.

We now demonstrate the electron holography capabilities of this setup. The JEOL biprism filament (0.6 µm in diameter) was positioned perpendicular to the insertion direction into the microscope column in order to minimize mechanical vibrations. **Figure 4**(a) shows both the fringe spacing and hologram width as a

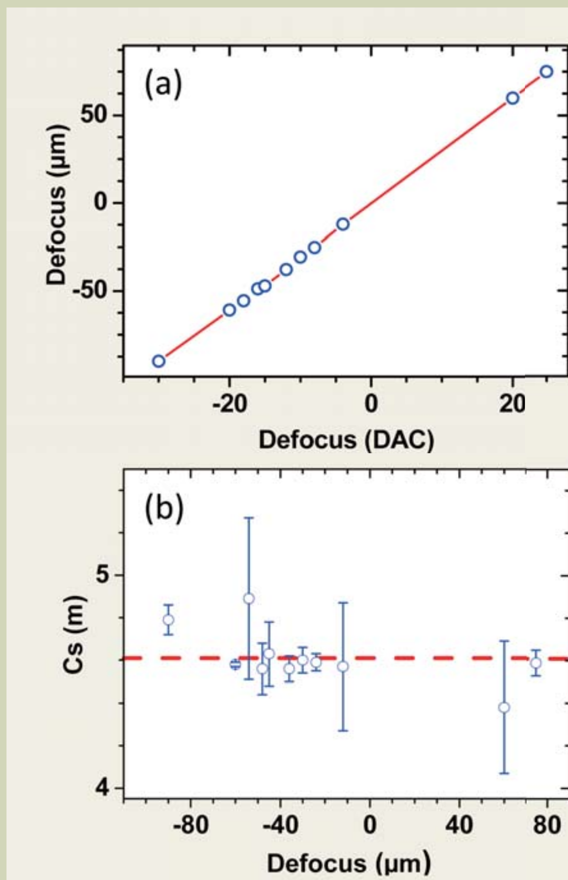

Fig. 2 (a) Defocus distance as a function of DAC setting of the objective mini-lens (b) coefficient of spherical aberration, Cs, measured at various defoci distances.

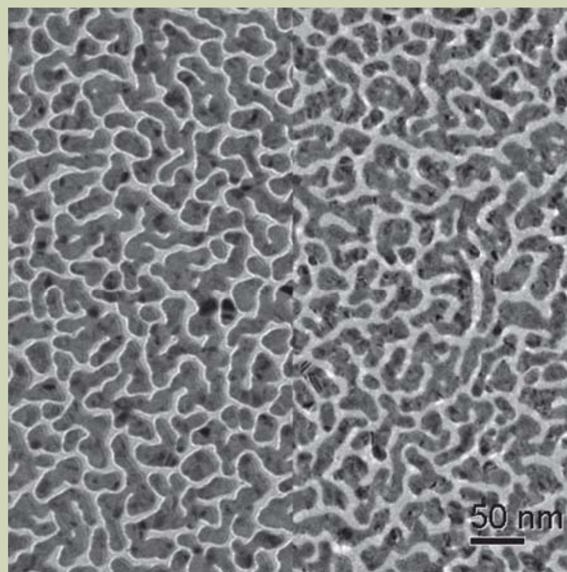

Fig. 3 Comparison of bright-field TEM imaging of gold nanoparticles on a carbon film recorded with the adapted Lorentz setting (left) and conventional imaging (right). The nominal magnification is 40kX.

function of applied voltage to the biprism. Figure 4(b) shows the contrast of these holograms, which in all cases was found to be over 10%. The acquisition time was set at 2 seconds. Longer recordings of holograms resulted in a deterioration of the contrast due to instabilities, mostly associated with the laboratory environment.

The holograms were recorded at a nominal magnification of 40kX. The width of the hologram that can be achieved in the low-magnification, Lorentz setting is larger than in regular TEM operation, reaching up to 1.2 µm. Such an increase may still not be sufficient for some magnetic imaging applications, for example when a large field of view across a thin film is required, or when the interaction between patterned elements or particles is examined.

Example: magnetic imaging of a patterned element

We demonstrate the magnetic imaging capabilities of the adapted Lorentz TEM on patterned magnetic elements. These elements were fabricated by depositing nominally 40 nm thick Permalloy ($Ni_{80}Fe_{20}$) films on Si_3N_4 membranes using electron-beam lithography and lift-off processing. Here, we show an example of a square element, with a side length of 0.5 µm. A bright-field image, obtained in the Lorentz mode, of this element, presented in **Figure 5**(a), highlights the polycrystalline structure of the Permalloy film. Figures 5(b,c) are Fresnel-contrast images, under- and over-focus, respectively, of 399 µm. Qualitatively, the bright and dark bands in the image, originating from domain walls, show a micromagnetic flux-closure structure. This structure can be characterized quantitatively by applying the 'Transport-of-Intensity' equation (TIE). The TIE is derived from a paraxial form of the flow conservation equation, which is obtained by applying the Schrödinger equation to an electron in a field-free region.[7, 8] Phase reconstructions were carried out using the Fourier transform-based approach of solving the TIE developed by Nugent *et al.,* (e.g. References [9, 10]) with the commercially available 'QPt' software.[11] Alignment of the defocused images was done using the 'Align 3_TP' plugin for ImageJ. [12]

An example of phase reconstruction for defocused images of 399 µm is shown in **Figure 6**(a). The result is presented in the form of an equiphase contour map,

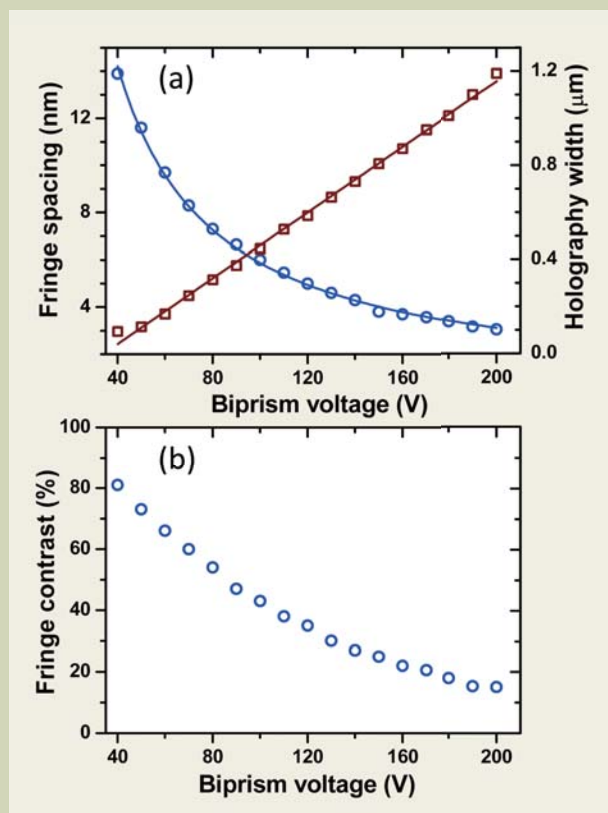

Fig. 4 Fringe spacing (a, left), off-axis hologram width (a, right), and fringe contrast (b) as a function of voltage applied to the biprism filament.

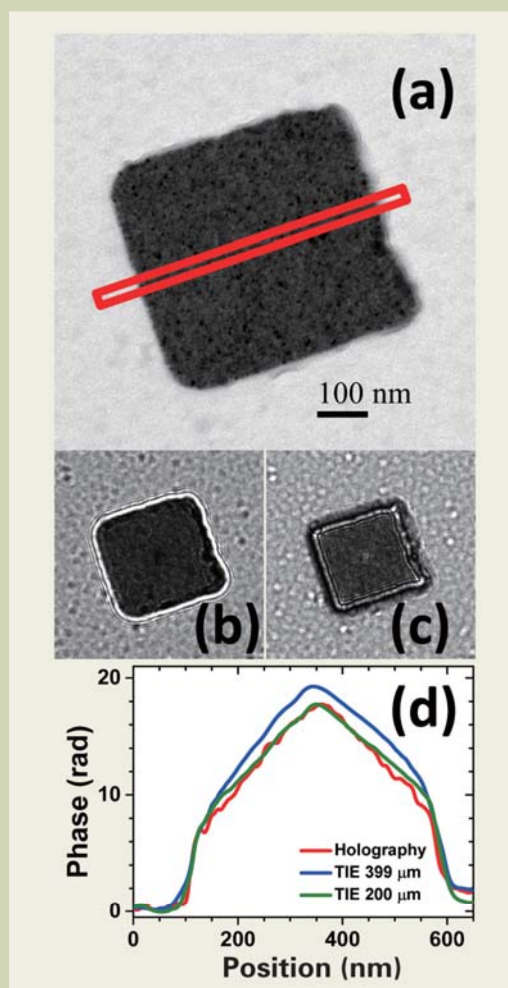

Fig. 5 (a) Bright-field TEM image of a nominally 40 nm thick square Permalloy element, 500 nm × 500 nm, patterned on a Si_3N_4 membrane. (b, c) Fresnel-contrast images, under-focus and over-focus, respectively, of 399 µm defocus distance. (d) Comparison of the reconstructed phase values along the direction denoted schematically by the red line in (a) for the off-axis holography measurements (red line) and the TIE phase reconstructions of Fresnel contrast images at 201 µm (green line) and 399 µm (blue line) defoci distances.

spaced at 1 radian between lines. This representation is convenient for magnetic mapping because the direction of the induction vector is along the equiphase line, and the magnitude of the vector is determined by the proximity of the contour lines (or gradient) perpendicular to the vector direction.

To test the reconstructed phase, we compare this result to off-axis electron holography measurements and Fresnel-contrast image simulations. Figure 6(b) is a phase-contour map of the same square Permalloy element measured by electron holography. Note that this result demonstrates two relative drawbacks compared to Fresnel-contrast imaging: the limited field of view, and the lack of a reference hologram from the vacuum, which degrades the quality of the reconstruction. Figure 6(c) is a phase-contour map calculated theoretically: The micromagnetic structure was first found by solving the time-dependent Landau-Lifshitz-Gilbert equations with the 'OOMMF' NIST package.[13] The magnetization distribution enables to determine the phase change of the electron wave. Following this, Fresnel-contrast Lorentz TEM images were simulated based on a code developed by McVitie *et al.*.[14] The calculation of the Fresnel-contrast images used here also include the optical parameters of this Lorentz TEM setting, the electrostatic potential of the sample, the change in amplitude of the electron wave due to the sample, and the shot-noise of the CCD. Finally, the phase was reconstructed from these simulated images using the TIE approach, shown in Figure 6(c).

A comparison of the phase values along the direction denoted schematically by the red line in Figure 5(a) is shown in Figure 5(d) for the off-axis holography measurements and the TIE reconstruction of Fresnel-contrast images at 201 μm and 399 μm. These phase line-scans show the typical electrostatic step at the edge of the element due to the change in the mean inner potential as well as the linear slopes within the sample due to the magnetic domain structure.

These comparisons are in agreement with the expected theoretical values, and show that quantitative magnetic mapping is indeed achieved to a good level in the adapted Lorentz TEM. Increasing the defocus distance increases the Fresnel contrast, which is useful for qualitative analysis. However, both the magnetic reconstruction and spatial resolution are degraded compared to reconstructions achieved with smaller defocus distances or electron holography.

Finally, an additional, indirect method to characterize the micromagnetic properties of the sample in the TEM is by low-angle electron diffraction (LAED). In this mode, the splitting of the central undiffracted beam is observed due to the Lorentz force. In the adapted JEOL JEM-2100F, this measurement was demonstrated by using 'free-lens control' of the intermediate lenses until the back-focal plane was observed on the viewing screen. **Figure 7** shows an example of a LAED obtained from a continuous Permalloy film sample, 45 nm thick. Figure 7(a) is a Fresnel-contrast image of a single domain region in the film showing typical ripple-contrast. The inset in the top left part of the image shows the central undiffracted beam in the back focal plane. In comparison, Figure 7(b) is a Fresnel-contrast image of a region including two magnetic domains. The domain wall is clearly visible as the white band, and the change of ripple-contrast on either side of the wall indicate the orientation of the magnetic moments within the domains. In this case, the LAED, shown in the inset in the top left hand corner of Figure 7(b) shows the splitting of the central beam. The deflection between the two spots is under 60 μrad, namely more than two orders of magnitude smaller than deflections measured for typical Bragg reflections.

Summary

Characterization of magnetic fields at the nanometer scale is important for the development of new materials

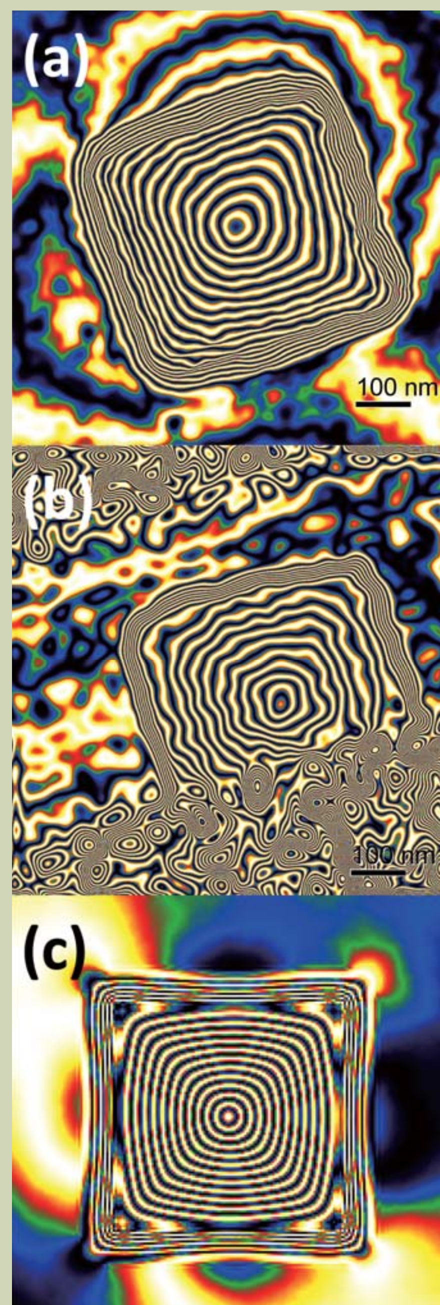

Fig. 6 Equiphase contour maps of the Permalloy square element derived from (a) TIE analysis of Fresnel-contrast images (399 μm defocus), (b) off-axis electron holography, (c) Fresnel-contrast image simulations from micromagnetic calculations, followed by phase reconstruction using the TIE approach. Note that the image simulations include specific characteristics of the adapted JEM-2100F for Lorentz TEM.

and devices. In this paper, we describe the adaptation of a conventional JEM-2100F to enable such measurements. Using a relatively simple and low-cost approach, Fresnel-contrast imaging is achieved while the sample is subjected to a field lower than 1 Oe during extended periods and over a wide range of microscope settings. Quantitative magnetic and electrostatic mapping of sub-micrometer magnetic structures at nanometer resolution has been demonstrated.

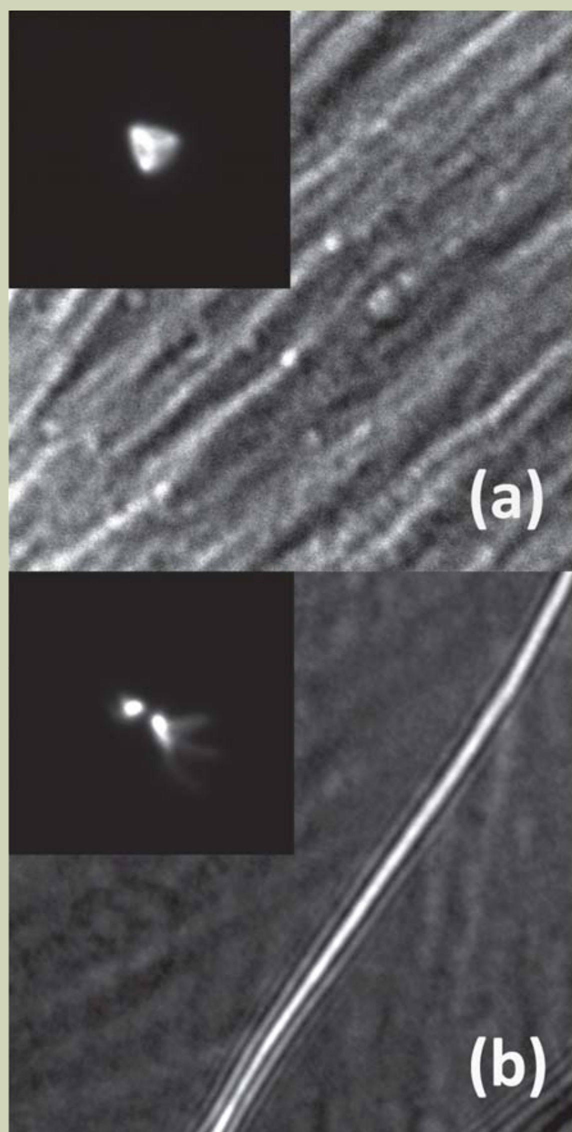

Fig. 7 Low-angle electron diffraction of a Permalloy film, 45 nm thick. (a) Fresnel-contrast image of a single domain region in the film (inset) LAED of this region (b) Fresnel-contrast image of a domain wall and two domain regions (inset) LAED of this region showing two spots at approximately 60 µrad separation.

Acknowledgments

The magnetic field neutralizer system was designed and built by Adrian Goodchild and Dave Greenshields in the Department of Physics, University of Warwick, UK.

We thank the assistance of Tom Hayward and Dan Allwood from the University of Sheffield, UK for supplying the lithographically patterned Permalloy elements.

The authors are grateful to Dorin Geiger and Hannes Lichte, Triebenberg Laboratory, Technische Universität Dresden, and Véronique Pierron-Bohnes and Corinne Ulhaq, Institut de Physique et de Chimie des Materiaux de Strasbourg for instruction and advise on off-axis electron holography.

We thank the technical assistance of JEOL (UK) Ltd., and AVBA Hitech Services, Israel.

References

[1] A. K. Petford-Long, A. Kohn, T. Bromwich, V. Jackson, F. Castano, and L. J. Singh, Application of TEM to the development of information storage materials, *Thin Solid Films*, **505** (1-2) 10-15 (2006) .

[2] A. Kohn, J. Dean, A. Kovacs, A. Zeltser, M. J. Carey, D. Geiger, G. Hrkac, T. Schrefl, and D. Allwood, Exchange-bias in amorphous ferromagnetic and polycrystalline antiferromagnetic bilayers: Structural study and micromagnetic modelling, *J. Appl. Phys.,* **109**(8) 083924 (2011).

[3] A. Kohn, C. Wang , A. K. Petford-Long , S. Wang, and R. C. C. Ward, Magnetization reversal processes in epitaxial Co/Fe bi-layers grown on MgO(001), *J. Appl. Phys.,* **103** (6) 063918 (1-9) (2008).

[4] M. A. Schofield, M. Beleggia, Y. Zhu, and G. Pozzi, Characterization of JEOL 2100F Lorentz-TEM for low-magnification electron holography and magnetic imaging, *Ultramicroscopy* **108** 625–634 (2008).

[5] M. A. Schofield, M. Beleggia, J. W. Lau, and Y. Zhu, Characterization of the JEM-2100F -LM TEM for Electron Holography and Magnetic Imaging, *JEOL news* **42** 2-7 (2007).

[6] O.L. Krivanek, *Optik* **45** 97 (1976).

[7] M. R. Teague, *J. Opt. Soc. Am.* **73**, 1434 (1983).

[8] A. Barty, D. Paganin, and K. Nugent, *in Magnetic Imaging and its Applications to Materials,* edited by M. De Graef and Y. Zhu, Academic Press, San Diego, 2001.

[9] D. Paganin and K. A. Nugent, *Phys. Rev. Lett.* **80** 2586 (1998).

[10] A. Kohn, A. K. Petford-Long, and T. C. Anthony, Determining the Magnetic Potential in Patterned Materials Using Energy-Dependent Lorentz Phase Microscopy, *Phys. Rev. B.* **72** 014444 (2005).

[11] QPt for Digital Micrograph, IATIA and HREM Inc.,

[12] W.S. Rasband, ImageJ, National Institutes of Health, Bethesda, Maryland, USA, http://rsb.info.nih.gov/ij/, 1997-2003. ; J. A. Parker, 'Align3_TP', Beth Israel Deaconess Medical Center Boston, Maryland, USA, http://www.med.harvard.edu/jpnm/ij/plugins/Align3TP.html

[13] M. J. Donahue and D. G. Porter, *OOMMF User's Guide*, Version 1.0 Interagency Report NISTIR 6376 National Institute of Standards and Technology, Gaithersburg, MD (Sept 1999).

[14] S. McVitie and M. Cushley, *Ultramicroscopy* **106** 423 (2006).